LANGMUIR

Article

pubs.acs.org/Langmuir

Self-Regulated Nanoparticle Assembly at Liquid/Liquid Interfaces: A Route to Adaptive Structuring of Liquids

Caili Huang,[†,‡] Mengmeng Cui,[‡] Zhiwei Sun,[‡] Feng Liu,[†] Brett A. Helms,*[,†,§] and Thomas P. Russell*[,†,‡,∥,⊥]

[†]Materials Sciences Division and [§]The Molecular Foundry, Lawrence Berkeley National Laboratory, One Cyclotron Road, Berkeley, California 94720, United States

[‡]Polymer Science and Engineering Department, University of Massachusetts, 120 Governors Drive, Conte Center for Polymer Research, Amherst, Massachusetts 01003, United States

[∥]Beijing Advanced Innovation Center for Soft Matter Science and Engineering, Beijing University of Chemical Technology, Beijing 100029, China

[⊥]WPI—Advanced Institute for Materials Research (WPI-AIMR), Tohoku University, 2-1-1 Katahira, Aoba, Sendai 980-8577, Japan

Supporting Information

ABSTRACT: The controlled structuring of liquids into arbitrary shapes can be achieved in biphasic liquid media using the interfacial assemblies of nanoparticle surfactants (NP-surfactants), that consist of a polar nanoparticle "head group" bound to one or more hydrophobic polymer "tails". The nonequilibrium shapes of the suspended liquid phase can be rendered permanent by the jamming of the NP-surfactants formed and assembled at the interface between the liquids as the system attempts to minimize the interfacial area between the liquids. While critical to the structuring process, little is known of the dynamic mechanical properties of the NP-surfactant monolayer at the interface as it is dictated by the characteristics of the component, including NP size and concentration and the molecular weight and concentration of polymers bound to the NPs. Here we provide the first comprehensive understanding of the dynamic mechanical character of two-dimensional NP-surfactant assemblies at liquid/liquid interfaces. Our results indicate that the dynamics of NP-polymer interactions are self-regulated across multiple time scales and are associated with specific mesoscale interactions between self-similar and cross-complementary components. Furthermore, the mechanical properties of the NP-surfactant monolayer are tunable over a broad range and deterministic on the basis of those component inputs. This control is key to tailoring the functional attributes of the reconfigurable structured liquids to suit specific applications.

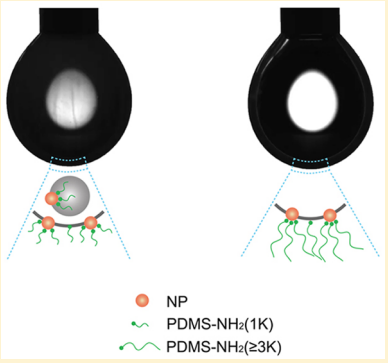

1. INTRODUCTION

The controlled structuring of liquids, in space and time, is a new frontier in soft matter science and engineering with profound implications for next-generation catalysis,[1−3] energy conversion,[4] additive manufacturing,[5] and nonequilibrium chemical systems.[6] An emerging and versatile strategy to structure a liquid within another involves the spontaneous assembly of nanoparticle surfactants (NP-surfactants) into a monolayer at the liquid/liquid interface. NP-surfactant monolayers form at the interface between two immiscible liquids when colloidal nanomaterials in one phase are held at the interface by polymers dissolved in the second phase, provided the polymer is modified with at least one functional group that is attracted to complementary functionality on the surface of the colloid; this process is concomitant with an overall reduction in the interfacial energy. Once this monolayer has formed, the structure of the interface (and therefore the liquids) can be sculpted into a variety of nonequilibrium structures using external fields (e.g., electric or shear). Such structured liquids hold their nonequilibrium shape indefinitely when NP-surfactants within the monolayer jam upon interfacial compression as the system attempts to revert to a shape with smaller interfacial area.[7,8]

Jamming behavior aside, the formation of a NP-surfactant monolayer involves multiple kinetic processes, including the diffusion of end-functionalized polymers and NPs from the bulk to the interface, the surface-diffusion of polymers and NPs, and the self-regulated process by which polymer chains bind to, stretch from, and distribute themselves across the surface of the NPs. Little is known how polymers engage in such self-regulation, or what the impact of polymer chain structure is on the mechanical attributes of the NP-surfactant monolayer, which are critical for generating a self-supporting structure once the system is jammed. Understanding how these mesostructure−property relationships are influenced by the physical dimensions of the NP is also unclear. Providing a framework to

Received: May 19, 2017
Published: July 18, 2017

DOI: 10.1021/acs.langmuir.7b01685
Langmuir 2017, 33, 7994−8001

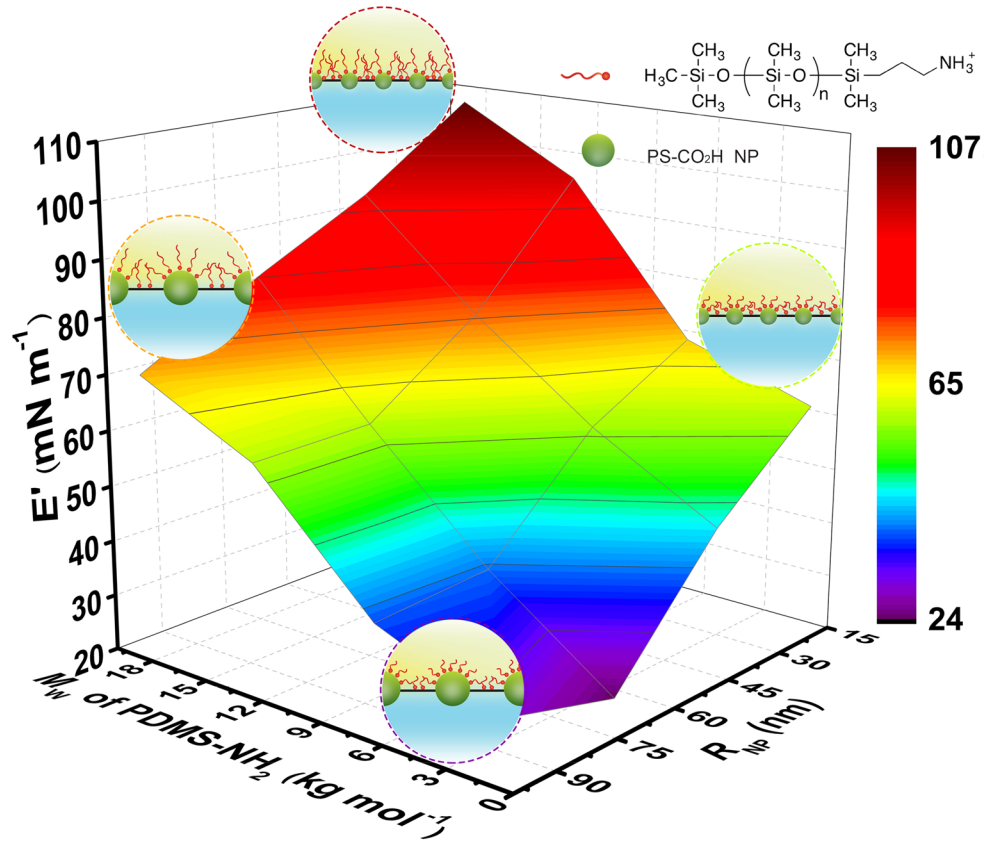

Figure 1. Storage modulus of a NP-surfactant interfacial assembly determined from oscillatory pendant drop experiments as a function of MW of PDMS-NH_2 and NP size at ν = 0.5 Hz, for a droplet consisting of a aqueous dispersion of PS-CO_2H NPs (0.1% w/w) suspended in toluene containing PDMS-NH_2 (0.0322 mmol L^{-1}) and the simple schematic representations of four corner interface cases.

assess these attributes quantitatively is key to understanding design rules for structuring liquids for target applications.

Here we present the first systematic study on the formation and assembly of NP-surfactants at liquid/liquid interfaces and highlight the dynamic mechanical properties of such interfacial NP-surfactant monolayer assemblies (Figure 1). Our results lay new foundations for structuring two immiscible liquids using responsive, reconfigurable, and interactive components in each phase. Our experimental design for this work focused on a key observation, that the rate of reduction in interfacial energy as NP-surfactants form competes with the compressive force arising from the continuous reduction in the interfacial area to reduce the free energy. Consequently, we hypothesized that the size and concentration of NPs, the molecular weight (MW) and concentration of the end-functionalized polymers, and the strength of the interactions between polymers and NPs should impact our ability to shape the liquids in a controlled manner. Indeed, we found that by varying these within specific ranges, the properties of NP-surfactants and higher-order monolayer assemblies could be tuned over a wide range, providing powerful new guidance to manipulate the system's quasi-2D structural properties across multiple length scales.

2. RESULTS AND DISCUSSION

Liquid/liquid interfaces provide a versatile platform to investigate two-dimensional (2D) assemblies of colloidal materials ranging in size from the nanoscopic to macroscopic length scales.[9−23] Driven by the reduction in the interfacial energy, monolayers of particles, whether they are amphiphilic or uniform in functionality, will form provided the sum of the interactions of the particles with the two immiscible fluids, normalized by the surface area of the particles, is less than the interactions between the two fluids. This forms the basis of the well-established Pickering emulsions.[24−30] Since the energetic gain per particle varies as the square of the particle radius, it follows that, as the size of the particles decreases, the reduction in the free energy holding the particle at the interface also decreases.

For particles that are microns to tens of microns in size, the energetic gain in placing the particles at the interface is substantive. Monolayer assemblies of large colloidal particles, provided the distribution of particle size is quite narrow, can even crystallize and any stretching or compression of the interfacial area will simply cause the colloidal assemblies to crack or buckle. For NPs, on the other hand, the energetic gain is considerably less, approaching thermal energies and their assemblies are generally more disordered, owing to the polydisperse character of many NP samples (by comparison to larger colloids). Both considerations contribute to the facile exchange of NPs between the interface and the fluid phase, and the assemblies are dynamic (i.e., mobile) in the plane of the interface. For these assemblies, if the interfacial area is decreased to increase the packing of the NPs at the interface, the compressive force resulting from the decreased area is sufficient to eject NPs into the surrounding liquid.[31]

To retain NPs at the interface under such conditions, we have recently shown that NPs functionalized with carboxylic acid groups on the surface and dispersed in an aqueous phase can interact with low-MW polymer chains having a complementary functionality, specifically an amine function-

DOI: 10.1021/acs.langmuir.7b01685
Langmuir 2017, 33, 7994−8001

ality, dissolved in an oil phase, such as toluene or silicon oil.[7,8] Polymer chains associate with NPs, forming NP-surfactants, having a polar NP "head" and multiple hydrophobic polymer chains as "tails". The number of chains attached to the NP is dynamic and ultimately self-regulated to maximize the reduction in interfacial energy. If the number is too small, NP-surfactants would eventually be drawn into the aqueous phase; if the number of anchored chains is too great, the NP-surfactants would be drawn into the oil phase.

Based on these considerations, the number of chains anchored to a NP of a given size at equilibrium can be expected to scale inversely with polymer MW. It may also be the case that increasing polymer MW also impacts the system dynamics, both with respect to the formation of polymer surfactants at the interface, and the reconfiguring of chains at the interface to minimize interfacial energy, both with and without NPs present in the aqueous phase. To understand the impact of polymer molecular weight on assembly outcomes, we secured or prepared amine-terminated polydimethylsiloxane (PDMS-NH_2) with MWs of ~1000 (1K), ~3000 (3K), ~7600 (7.6K), and ~18900 (18.9K) g mol^{-1} using organocatalytic anionic ring-opening polymerization[32] from 6-azidohexan-1-ol and straightforward polymer end-group manipulation (see Supporting Information).

Using dynamic pendant-drop tensiometry, we determined the rate of reduction in the interfacial tension (IFT) and the IFT at equilibrium for systems configured with water droplets immersed in toluene containing PDMS-NH_2 of varying MW at a constant molar fraction (1.61 mmol L^{-1}; Figure 2a). The initial rate at which the IFT decreased was found to decrease with increasing MW. Characteristic decay times of 327, 495, and 517 s, were calculated for 3K, 7.6K, and 18.9K PDMS-NH_2, respectively, assuming a single exponential decay; the diffusion of 1K PDMS-NH_2 to the interface was too rapid to measure in the pendant drop geometry. For long times, where the systems were approaching equilibrium, the IFT decreased with increasing polymer MW from 27.4 (1K PDMS-NH_2) to 26.2, 25.1, and 22.4 mN m^{-1}. Since the experiments were performed at a constant molar concentration of polymer (1.61 mmol L^{-1}), the total number of polymer chains in solution was constant, underscoring the increased effectiveness of individual chains in reducing water/toluene contacts.

For each of the PDMS-NH_2 surfactants with varying MW, we found that the IFT at equilibrium for a water/toluene interface decreased with increasing concentration of the polymer (Figure 2b). Furthermore, the rate at which the IFT initially decreased was found to increase with higher concentrations of PDMS-NH_2, regardless of polymer MW (Figure 2e). These kinetic data suggest that the behavior of the system is dominated by the influence of polymer surfactant concentration on the average distance a polymer must diffuse to reach the water/toluene interface, which decreases with higher concentrations of the polymer. Notable too was the extent to which IFT at equilibrium varied with polymer concentration (Figure 2f); for example, an IFT of 34.6 mN m^{-1} was measured for the water/toluene interface configured with the 3K PDMS-NH_2 surfactant at a concentration of 0.0322 mmol L^{-1}, whereas for 16.1 mmol L^{-1}, the IFT dropped considerably to ~19 mN m^{-1}. Here, the differences in IFT with polymer concentration are reflecting the tendency of the system to balance the chemical potentials of the chains adsorbed at the interface with those chains dissolved in the toluene. In other words, with increasing concentration of the polymer surfactant, more chains absorb at the water/toluene interface more rapidly.

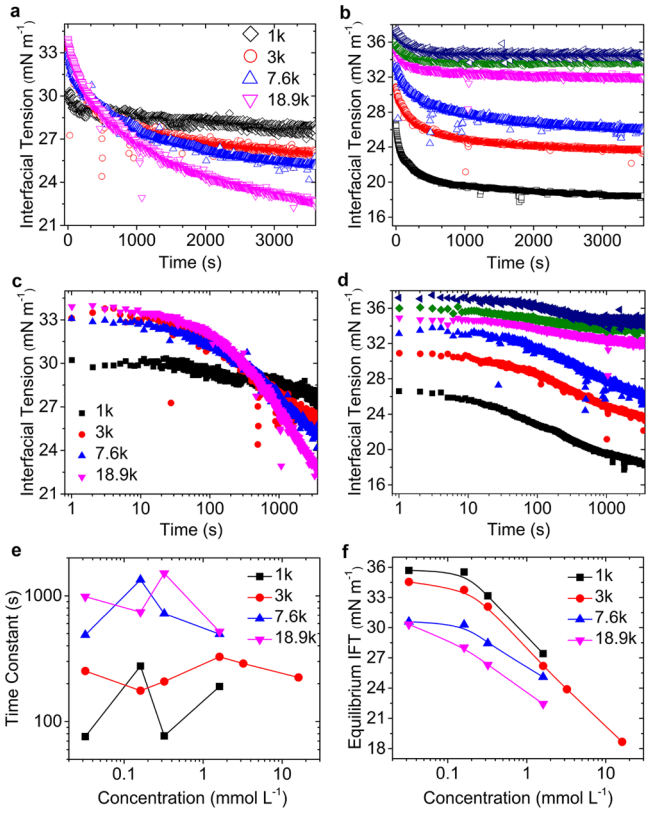

Figure 2. (a) IFT, as measured by pendant drop tensiometry, vs time for an aqueous droplet suspended in toluene containing PDMS-NH_2 (MW = 1K, 3K, 7.6K, or 18.9K; concentration = 1.61 mmol L^{-1}). (b) IFT vs time for an aqueous droplet suspended in toluene containing 3K PDMS-NH_2 of varying concentration (from top to bottom: 0.0322, 0.161, 0.322, 1.61, 3.22, and 16.1 mmol L^{-1}). (c) Logarithmic representation of the data in (a). (d) Logarithmic representation of the data in (b). (e) Time constants and (f) equilibrium IFT of different MW polymers as a function of concentration.

Having quantified the kinetic profiles for PDMS-NH_2 assembly at the water/toluene interface, we then introduced PS-CO_2H NPs into the aqueous phase and established the role of NP size and concentration on the rate of NP-surfactant (and NP-surfactant monolayer) formation at the interface, where the molecular weight and concentration of the PDMS-NH_2 were varied. It should be noted that PS-CO_2H NPs are not interfacially active.[8] We first considered a system consisting of an aqueous dispersion of 16.5 nm PS-CO_2H NPs (0.1% *w*/*w*) in contact with toluene containing 3K PDMS-NH_2 at different concentrations (Figure 3a). Here, the rate of reduction in IFT increased with higher concentrations of 3K PDMS-NH_2, such that for concentrations in excess of 3.22 mmol L^{-1}, the rate was too rapid to measure with the tensiometer. In all instances, after the initial reduction in IFT, there is a second slower process that leads to a continued slight decrease in IFT with time. We attribute this slow process to the rearrangement of NP-surfactants at the interface. Notably, all IFT end-points were at values considerably lower than those in the absence of PS-CO_2H NPs, highlighting the significant gains in free energy associated with NP-surfactant formation and their assembly into monolayers at the interface. As the MW of PDMS-NH_2 was increased beyond 3K (see Figures S6–S8), the same

DOI: 10.1021/acs.langmuir.7b01685
Langmuir 2017, 33, 7994–8001

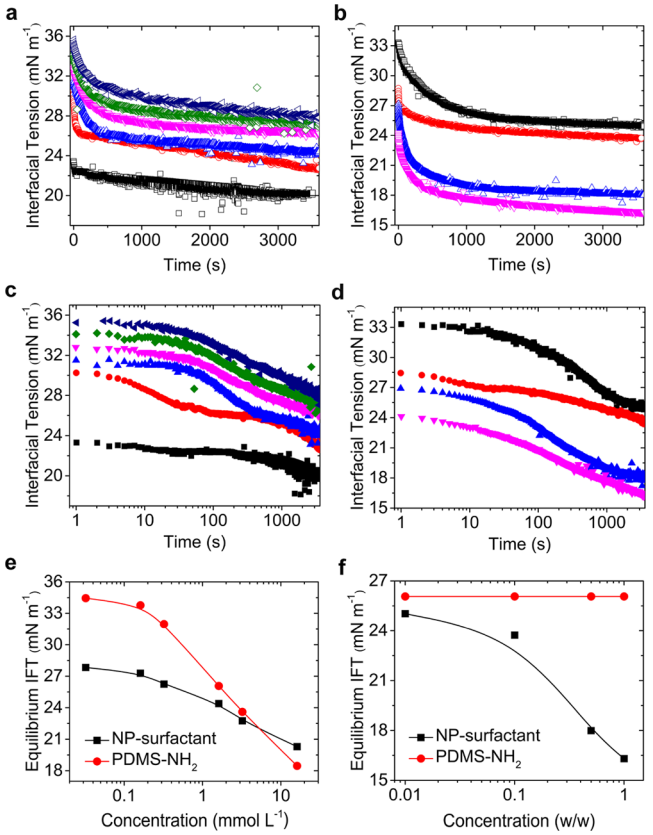

Figure 3. (a) IFT vs time for pendant droplets consisting of an aqueous dispersion of PS-CO_2H NPs (0.1% *w*/*w*) that were immersed in toluene containing 3K PDMS-NH_2 of varying concentration (from top to bottom: 0.0322, 0.161, 0.322, 1.61, 3.22, and 16.1 mmol L^{-1}). (b) IFT vs time for pendant droplets consisting of an aqueous dispersion of PS-CO_2H NPs of varying concentration (from top to bottom: 0.01, 0.1, 0.5, 1.0% *w*/*w*) that were immersed in toluene containing 3K PDMS-NH_2 (1.61 mmol L^{-1}). (c) Logarithmic representation of the data in (a). (d) Logarithmic representation of the data in (b). (e) Equilibrium IFT of NP-surfactants, from (a), relative to the 3K PDMS-NH_2 alone as a function of polymer concentration. (f) Equilibrium IFT of NP-surfactants, from (b), relative to the 3K PDMS-NH_2 alone as a function of NP concentration.

general trends were observed, but the rates were found to decrease with increasing PDMS-NH_2 MW, as would be expected from the decrease in the diffusion coefficient for higher MW polymers. Finally, we noted that the absolute value of the equilibrium IFT decreased with increasing PDMS-NH_2 MW, to values less than 18 mN m^{-1} in some cases.

If, on the other hand, the MW of PDMS-NH_2 was fixed at 3K and its concentration kept constant at 1.61 mmol L^{-1} and the concentration of 16.5 nm PS-CO_2H NPs varied, the results in Figure 3b were obtained. For low concentrations of 16.5 nm PS-CO_2H NPs (<0.1% *w*/*w*), the reduction in IFT is gradual, with a characteristic time of 1144 s. This clearly reflects the diffusion of NPs to the interface, the sticking of NPs at the interface by interactions with end-functionalized polymers, and the reorganization necessary for subsequent NPs to be anchored to the interface. However, as the concentration of the NPs is increased, the reduction in the IFT is much more rapid, with a characteristic time of 214 s, and the equilibrium reduction in the IFT is much more significant, to values of 16 mN m^{-1}.

The MW of PDMS-NH_2 also played an important role in the formation of NP-surfactants and their ultimate behavior in time and in space. More specifically, we found that if the MW of PDMS-NH_2 is increased and the concentration varied to keep the number of functional groups constant, and the diameter and concentration of the PS-CO_2H NPs were held constant at 16.5 nm and 0.1% *w*/*w*, respectively, then the initial rate of reduction in the IFT decreased with increasing MW of the polymer due, primarily, to the reduction in the rate of diffusion of the ligand to the interface (Figures 4a and 2e). The equilibrium IFT was also found to decrease with increasing polymer MW, down to values of 16 mN m^{-1} or less. A curious behavior, however, was observed for the 1K PDMS-NH_2. Shown in Figure 4c are photographs of four pendant droplets, each acquired after the droplets were left in contact with a solution of PDMS-NH_2 (of varying MW) in toluene for a period of 1 h. Droplets formed using 3K, 7.6K, and 18.9K PDMS-NH_2 (1.61 mmol L^{-1}) in the toluene phase with a 16.5 nm diameter PS-CO_2H NPs (0.1% *w*/*w*) in the aqueous phase were stable for up to 24 h. However, for droplets generated using a solution of 1K PDMS-NH_2 (1.61 mmol L^{-1}) in toluene, the droplet became cloudy within 1 h and, after standing overnight, became opaque. The shape of the droplet did not change; however, it was evident that micelles had formed in the aqueous phase and that the concentration of micelles increased over time. The micelles were quite mobile within the aqueous phase and did not preferentially segregate to the top or the bottom of the water droplet, suggesting that they are buoyant in the water phase. While the exact origin of these micelles is not known, we speculate that these arise from instabilities at the water/toluene interface and that the short length of the PDMS chain is not sufficiently long to anchor the chain solidly in the toluene phase, that is, fluctuations at the water/toluene interface are not sufficiently suppressed and can grow into droplets that bud-off and are drawn into aqueous phase. A similar behavior was observed previously with amphiphilic block copolymers at the water/oil interface.[33]

Finally, we turn to the influence of the size of the NPs constituting the headgroup of these NP-surfactants on the assembly process and associated system dynamics. Keeping the MW and concentration of PDMS-NH_2 fixed at 3K and 1.61 mmol L^{-1}, respectively, and the concentration of PS-CO_2H NPs fixed (0.1% *w*/*w*) but the particle diameter allowed to vary from 16.5–97 nm, we noted that, with increasing NP diameter, the rate at which the IFT decreased was found to increase (Figure 4e). Based simply on the size of the NPs, this result presents a conundrum, since the NPs must diffuse to the interface and interact with the end-functionalized polymers assembled at the interface. In addition, since the weight fraction of the NPs was kept fixed, as the diameter of the NPs increases the total number of number of NPs will decrease by the cube of the radius (i.e., NP volume). Furthermore, the absolute values for IFT decreased markedly with increasing NP size. Per NP, the extent to which IFT is expected to decrease will necessarily increase with NP size; this reflects the area occupied at the interface by each NP. These results indicate that, even though the number of NPs adsorbing at the interface per unit time decreased with increasing NP size, the reduction in the IFT per particle appears to control the rate at which the IFT decreases. In other words, the larger the NP, the greater will be the reduction in the IFT. This may stand counter to the argument that as the NP size increases, the interstitial area between the NPs increases, exposing more interface. However, the end-

DOI: 10.1021/acs.langmuir.7b01685
Langmuir 2017, 33, 7994–8001

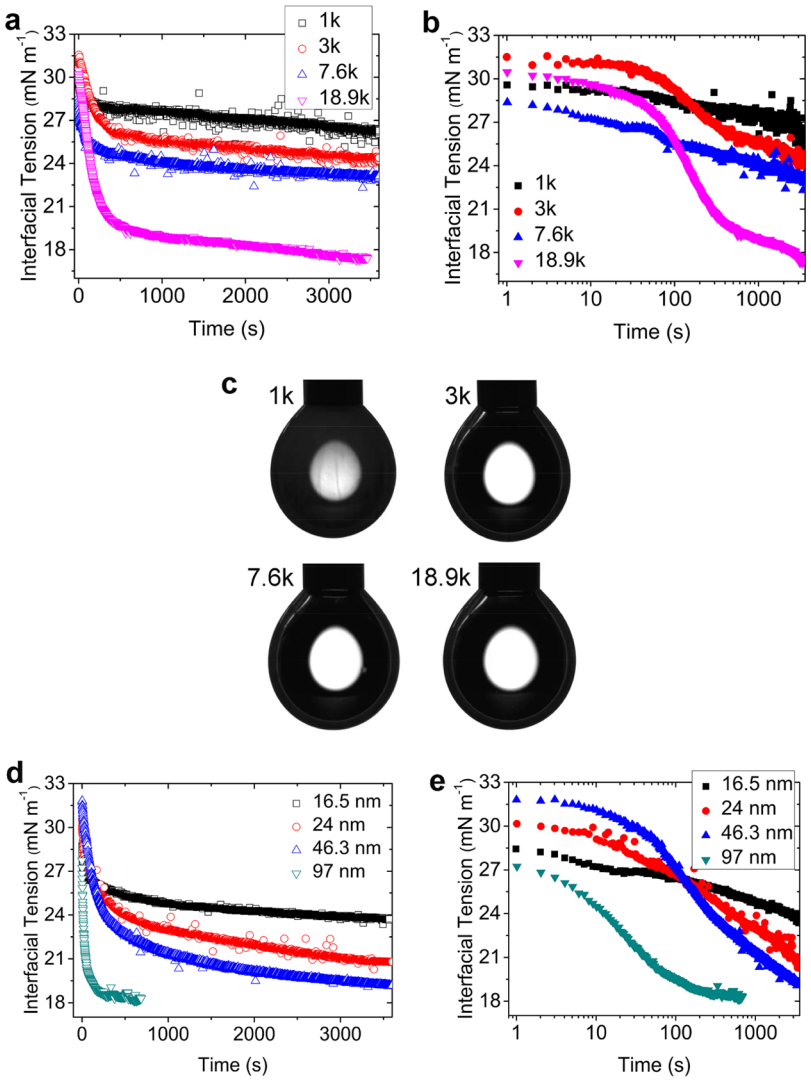

Figure 4. (a) IFT vs time for pendant droplets consisting of an aqueous dispersion of PS-CO_2H NPs (0.1% *w*/*w*) that were immersed in toluene containing PDMS-NH_2 of varying MW at a constant molar concentration (1.61 mmol L^{-1}). (b) Logarithmic representation of the data in (a). (c) Photographs of pendant droplets of aqueous dispersions of PS-CO_2H NPs (0.1% *w*/*w*) after the droplets were left in contact with a solution of PDMS-NH_2 (of varying MW) in toluene for a period of 1 h. (d) IFT vs time for pendant droplets consisting of an aqueous dispersion of PS-CO_2H NPs of varying size at a constant concentration (0.1% *w*/*w*) that were immersed in toluene containing 3K PDMS-NH_2 (1.61 mmol L^{-1}) (e) Logarithmic representation of the data in (d).

functionalized polymer will still have assemble at this interstitial area. Consequently, the penalty for exposing this area is significantly reduced.

One of the outstanding questions associated with the properties of a monolayer of NP-surfactants, regardless of the components used, is related to how the structure of such an assembly at the liquid/liquid interface is responsive to perturbations. Multiple interactions, including polymer−polymer, NP−polymer, and NP−NP interactions, ultimately dictate the system's response. All of those interactions will depend strongly on the selection of components with respect to size or molecular weight, as well as their respective concentrations in each phase. Interfacial dilatational rheology probes the stress−strain response of films at liquid/liquid and air/liquid interfaces subject to deformation conditions similar to those used in bulk rheology. Such interfacial rheological properties have been correlated with the stability of emulsions and foams.[34−38] When a fluid−fluid interface in any of these systems (or one such as ours) is driven out of equilibrium by an expansion or contraction in the area, a dilatational strain is generated; in turn, relaxations will return the interface to its equilibrium state. Both structural relaxations and exchange of components at the interface with the surrounding fluid can give rise to these relaxations.

In an oscillatory dilatational rheology experiment, if the interfacial dilatational strain falls within the linear viscoelastic regime, rheological properties can be obtained in the frequency (ω)-dependent dilatational complex modulus $E^*(\omega)$, which can be broken down into a real (storage) and imaginary (loss) component, $E'(\omega)$ and $E''(\omega)$, respectively, from which the phase angle δ is determined,

$$E^*(\omega) = E'(\omega) + i\omega E''(\omega) \quad (1)$$

$$\tan \delta(\omega) = E''(\omega)/E'(\omega) \quad (2)$$

These two-dimensional dilatational moduli have fundamental units of [mass·time^{-2}], also expressed as [energy·area^{-1}] or [force·length^{-1}]. $E^*(\omega)$ is calculated

DOI: 10.1021/acs.langmuir.7b01685
Langmuir 2017, 33, 7994−8001

$$E^*(\omega) = \frac{d\gamma}{d \ln A} \quad (3)$$

as the area A oscillates sinusoidally with amplitude ΔA about initial area A_0,

$$A(t) = A_0 + \Delta A \exp(i\omega t) \quad (4)$$

and the measured surface tension $\gamma(t)$ oscillates about the static surface tension γ_0 with amplitude $\Delta\gamma(\omega)$,

$$\gamma(t) = \gamma_0 + \Delta\gamma(\omega)\exp[i(\omega t + \delta(\omega))] \quad (5)$$

For all cases investigated, regardless of PS-CO_2H NP size and concentration, or the concentration and molecular weight of PDMS-NH_2, two transitions in E', two peaks in E'' and, correspondingly, two maxima in δ were observed: one at high frequencies and one at low frequencies, as shown in Figure 5

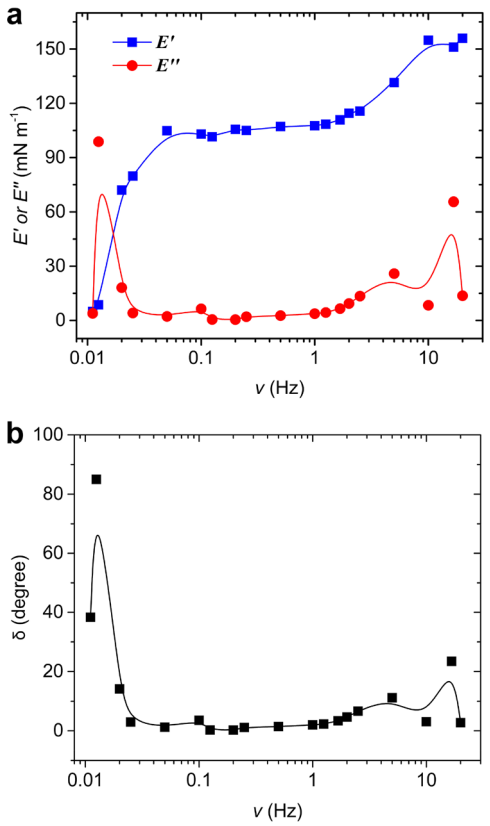

Figure 5. (a) Storage and loss moduli of a NP-surfactant interfacial assembly determined from oscillatory pendant drop experiments as a function of frequency, ν, for a droplet consisting of an aqueous dispersion of 16.5 nm PS-CO_2H NPs (0.1% w/w) suspended in toluene containing 18.9K PDMS-NH_2 (0.0322 mmol L^{-1}). (b) Phase angle (δ) determined from E' and E''.

for a droplet consisting of an aqueous dispersion of 16.5 nm PS-CO_2H NPs (0.1% w/w) suspended in a solution of 18.9K PDMS-NH_2 in toluene (0.0322 mmol L^{-1}). In the intermediate frequency range, E' was constant ~105 mN m^{-1}, reflecting the elastic character of the NP-surfactant assemblies. E'' was also constant over this frequency range but $E' \gg E''$, again reflecting the elastic nature of the assemblies. Surprisingly, these plateau regions were independent of the MW of PDMS-NH_2, indicating that the entanglement of PDMS chains associated with the NPs did not play a significant role in the relaxation of the NP-surfactant assemblies. This, more than likely, can be attributed to the low MW of the PDMS chains associated with the NPs and the excellent solubility of PDMS-NH_2 in toluene. We attribute the transition in the high frequency regime to a transition in the interactions between NPs and ligands attached to the NPs, while at low frequencies a disengagement of PDMS-NH_2 attached to adjacent NPs occurs. Neither feature is seen with only PDMS-NH_2 at the interface, where E' fluctuated by only several mN m^{-1}.[39]

As shown in Figure S9, the elastic modulus, corresponding to the plateau in the intermediate frequency range, decreased from ~60 mN m^{-1} to 35 mN m^{-1} with an increase in 3K PDMS-NH_2 concentration from 0.0322 to 1.61 mmol L^{-1}, for a fixed concentration (0.1% w/w) of 16.5 nm PS-CO_2H NPs in the aqueous phase. This decease arises from the ability of free 3K PDMS-NH_2 to exchange with the surrounding medium, which will increase in likelihood with higher polymer concentrations. When the concentration of 3K PDMS-NH_2 was fixed at 0.0322 mmol L^{-1}, E' of NP-surfactant film at the interface was constant, regardless of the NP concentration (Figure S10). Unlike the free PDMS-NH_2 in the system, NPs cannot easily exchange with NPs in the surrounding aqueous medium. Furthermore, as the size of PS-CO_2H NPs increases, at a fixed concentration of PS-CO_2H (0.1% w/w) and 3K PDMS-NH_2 (0.0322 mmol L^{-1}), E' was found to decrease (Figure S11). More than likely, this arises from the larger interstitial regions between NPs and the higher concentration of free polymer that can exchange with the surrounding medium. Figure S12 shows that E' decreased from 105 mN m^{-1} to 60 mN m^{-1} as the MW of the PDMS-NH_2 was decreased from 18.9K to 4K, and then remained constant at ~60 mN m^{-1} as the MW was further decreased. This trend can be attributed to the ability of NP-associated (i.e., bound) 18.9K PDMS-NH_2 to interact with each other. These results suggest that the elasticity of NP-surfactant assemblies could be significantly increased with much higher MW PDMS-NH_2 attached to the NPs. Our findings demonstrate that the elasticity of the NP-surfactant assembled film can be tuned independent of either the MW of PDMS-NH_2 or the NP size over a wide range (Figure 1). If, though, the PDMS were functionalized on both ends of the chain (i.e., H_2N-PDMS-NH_2), one PDMS molecule can associate with two adjacent NPs, which should significantly increase E' for the assembly. Indeed, as shown in Figure S13, E' in the intermediate frequency range increased from 60 mN m^{-1} to 80 mN m^{-1}, keeping the molar concentration of the amine groups the same. This opens a different avenue by which the NP assemblies can be stabilized while being perturbed.

3. CONCLUSIONS

The assembly and properties of responsive and reconfigurable colloidal NP-surfactants, generated by the interaction between an aqueous dispersion of carboxylic-acid functionalized polymeric NPs and a solution of amine end-functionalized PDMS in toluene, were investigated as a function of NP size and concentration and PDMS molecular weight and concentration. The reduction in the interfacial tension and the rate at which the reduction occurred was found to depend on each of these parameters. Using difunctional PDMS chains, it is apparent that the NP-surfactant assemblies can be cross-linked, locking in a nonequilibrium, mesoscopic shape. We quantified both the storage and loss moduli of the assemblies, determined from oscillatory pendant drop studies, which show that the elastic modulus can be increased either by increasing the molecular weight of the PDMS chains or by cross-linking the

DOI: 10.1021/acs.langmuir.7b01685
Langmuir 2017, 33, 7994−8001

NP-surfactant assemblies with difunctional PDMS chains. These results point to strategies by which real-time changes in the shape of a liquid can be kinetically trapped in nonequilibrium mesoscopic shapes by using a combination of low molecular weight ligands to rapidly associate with the NPs at the interface followed by a slower diffusion of higher molecular weight chains to the interface and exchanging with the lower molecular weight chains to reduce the interfacial tension and increase the elastic modulus of the assembly.

4. EXPERIMENTAL SECTION

Materials. Cross-linked PS-CO_2H nanoparticles (diameter: 16.5, 24, 46.3, and 97 nm) were obtained as an aqueous dispersion from Microspheres-Nanospheres (Cold Spring, New York). Monoamino-terminated polydimethylsiloxane (PDMS-NH_2, MW = 1000 or 3000 g mol^{-1}) and diamino-terminated polydimethylsiloxane (NH_2−PDMS-NH_2, MW = 2500 g mol^{-1}) were purchased from Polymer Source and Sigma-Aldrich, respectively. All other PDMS-NH_2 materials were synthesized using organocatalytic ring-opening polymerization.[40,41] 6-Bromo-1-hexanol, sodium azide (NaN_3), triphenylphosphine (PPh_3), and benzoic acid were purchased from Sigma-Aldrich and used as received. 1,5,7-Triazabicyclo[4.4.0]dec-5-ene (TBD) was purchased from purchased from Sigma-Aldrich and purified by bulb-to-bulb distillation using a Kugelrohr apparatus. 2,2,4,4,6,6-Hexamethylcyclotrisiloxane (D_3) was purchased from Gelest and distilled over calcium hydride under nitrogen atmosphere. Anhydrous and degassed acetonitrile (ACN) was collected from a J. D. Meyer solvent purification system. Deionized water was obtained from a Milli-Q water purification system.

Characterization. ^1H NMR spectra were recorded using a Bruker Biospin spectrometer in $CDCl_3$. Fourier Transform Infrared spectroscopy (FT-IR) measurements were performed on a PerkinElmer Spectrum One spectrometer. The interfacial tension between water and the organic solvent, and the rheological properties of water/oil interface were measured with a tensiometer (Krüss DSA30S) by the pendant drop method and oscillating model, respectively. The volume of the droplets was kept constant at 30 μL.

Assembly of NP Surfactant at the Water/Toluene Interface. An interface was created by injecting a pendent drop of PS-CO_2H NPs in water into a toluene solution containing PDMS-NH_2 or H_2N-PDMS-NH_2. The physical attributes of the droplet were monitored over time by recording the interfacial tension. The rheological properties of the NP-surfactant monolayer assembly at the interface, after equilibrium coverage had been reached, were determined by an oscillatory dilation of the interfacial area, measuring the in-phase and out-of-phase component of the interfacial tension (γ). The sinusoidal deformation of the surface area ($\Delta A/A_0$) was kept at ∼2% to remain within the linear viscoelastic regime. The interfacial tension and surface area of a droplet were measured as a function of time (typical example: Figure S5) over the entire accessible frequency range (0.01−20 Hz). The interfacial tension remained constant (to within 0.5 mN m^{-1}) before and after the oscillatory measurements. Different concentrations and MW of PDMS-NH_2 or H_2N-PDMS-NH_2 were used. For 3K PDMS-NH_2, concentrations of 0, 0.01, 0.05, 0.1, 0.5, 1 and 5% v/v were used, and the same molar concentration of amine was kept constant when using other MWs of the polymer (i.e., 1K, 4K, 7.6K, 12.7K, or 18.9K PDMS-NH_2). For these experiments, the concentration of PS-CO_2H NPs was varied from 0.01% w/w to 0.1, 0.5, and 1% for each of the different particle sizes (i.e., 16.5, 24, 46.3, and 97 nm diameters).

■ ASSOCIATED CONTENT

Supporting Information

The Supporting Information is available free of charge on the ACS Publications website at DOI: 10.1021/acs.langmuir.7b01685.

Synthesis of PDMS-NH_2 (Scheme S1, Figures S1−S4) as well as IFT and rheological properties of NP-surfactant monolayer assembly (Figures S5−S13; PDF).

■ AUTHOR INFORMATION

Corresponding Authors

*E-mail: bahelms@lbl.gov.
*E-mail: tom.p.russell@gmail.com.

ORCID

Caili Huang: 0000-0003-1209-1141
Brett A. Helms: 0000-0003-3925-4174
Thomas P. Russell: 0000-0001-6384-5826

Notes

The authors declare no competing financial interest.

■ ACKNOWLEDGMENTS

This work was supported by the U.S. Department of Energy, Office of Science, Office of Basic Energy Sciences, Materials Sciences and Engineering Division under Contract No. DE-AC02-05-CH11231 within the Adaptive Interfacial Assemblies Towards Structuring Liquids program (KCTR16). Portions of the work, including polymer synthesis and characterization, were carried out as a User Project at the Molecular Foundry, which is supported by the Office of Science, Office of Basic Energy Sciences, of the U.S. Department of Energy under Contract No. DE-AC02-05CH11231.B. A.H. acknowledges additional support from the Office of Science, Office of Basic Energy Sciences, of the U.S. Department of Energy under the same contract.

■ REFERENCES

(1) Myers, R. M.; Fitzpatrick, D. E.; Turner, R. M.; Ley, S. V. Flow Chemistry Meets Advanced Functional Materials. *Chem. - Eur. J.* **2014**, *20*, 12348−12366.

(2) Wegner, J.; Ceylan, S.; Kirschning, A. Flow Chemistry - a Key Enabling Technology for (Multistep) Organic Synthesis. *Adv. Synth. Catal.* **2012**, *354*, 17−57.

(3) McQuade, D. T.; Seeberger, P. H. Applying Flow Chemistry: Methods, Materials, and Multistep Synthesis. *J. Org. Chem.* **2013**, *78*, 6384−6389.

(4) Weber, A. Z.; Mench, M. M.; Meyers, J. P.; Ross, P. N.; Gostick, J. T.; Liu, Q. Redox Flow Batteries: a Review. *J. Appl. Electrochem.* **2011**, *41*, 1137−1164.

(5) Melchels, F. P. W.; Domingos, M. A. N.; Klein, T. J.; Malda, J.; Bartolo, P. J.; Hutmacher, D. W. Progress in Polymer Science. *Prog. Polym. Sci.* **2012**, *37*, 1079−1104.

(6) Hermans, T. M.; Stewart, P. S.; Grzybowski, B. A. pH Oscillator Stretched in Space but Frozen in Time. *J. Phys. Chem. Lett.* **2015**, *6*, 760−766.

(7) Cui, M.; Emrick, T.; Russell, T. P. Stabilizing Liquid Drops in Nonequilibrium Shapes by the Interfacial Jamming of Nanoparticles. *Science* **2013**, *342*, 460−463.

(8) Huang, C.; Sun, Z.; Cui, M.; Liu, F.; Helms, B. A.; Russell, T. P. Structured Liquids with pH-Triggered Reconfigurability. *Adv. Mater.* **2016**, *28*, 6612−6618.

(9) Lin, Y.; Skaff, H.; Emrick, T.; Dinsmore, A. D.; Russell, T. P. Nanoparticle Assembly and Transport at Liquid-Liquid Interfaces. *Science* **2003**, *299*, 226−229.

(10) Lin, Y.; Böker, A.; Skaff, H.; Cookson, D.; Dinsmore, A. D.; Emrick, T.; Russell, T. P. Nanoparticle Assembly at Fluid Interfaces: Structure and Dynamics. *Langmuir* **2005**, *21*, 191−194.

(11) Böker, A.; He, J.; Emrick, T.; Russell, T. P. Self-Assembly of Nanoparticles at Interfaces. *Soft Matter* **2007**, *3*, 1231−1248.

(12) Stratford, K. Colloidal Jamming at Interfaces: a Route to Fluid-Bicontinuous Gels. *Science* **2005**, *309*, 2198−2201.

DOI: 10.1021/acs.langmuir.7b01685
Langmuir 2017, 33, 7994−8001

(13) Herzig, E. M.; White, K. A.; Schofield, A. B.; Poon, W. C. K.; Clegg, P. S. Bicontinuous Emulsions Stabilized Solely by Colloidal Particles. *Nat. Mater.* **2007**, *6*, 966−971.
(14) Tavacoli, J. W.; Thijssen, J. H. J.; Schofield, A. B.; Clegg, P. S. Novel, Robust, and Versatile Bijels of Nitromethane, Ethanediol, and Colloidal Silica: Capsules, Sub-Ten-Micrometer Domains, and Mechanical Properties. *Adv. Funct. Mater.* **2011**, *21*, 2020−2027.
(15) Walther, A.; Matussek, K.; Müller, A. H. E. Engineering Nanostructured Polymer Blends with Controlled Nanoparticle Location Using Janus Particles. *ACS Nano* **2008**, *2*, 1167−1178.
(16) Bahrami, R.; Löbling, T. I.; Gröschel, A. H.; Schmalz, H.; Müller, A. H. E.; Altstädt, V. The Impact of Janus Nanoparticles on the Compatibilization of Immiscible Polymer Blends Under Technologically Relevant Conditions. *ACS Nano* **2014**, *8*, 10048−10056.
(17) Fujii, S.; Randall, D. P.; Armes, S. P. Synthesis of Polystyrene/Poly[2-(Dimethylamino)Ethyl Methacrylate- Stat-Ethylene Glycol Dimethacrylate] Core−Shell Latex Particles by Seeded Emulsion Polymerization and Their Application as Stimulus-Responsive Particulate Emulsifiers for Oil-in-Water Emulsions. *Langmuir* **2004**, *20*, 11329−11335.
(18) Zhang, J.; Coulston, R. J.; Jones, S. T.; Geng, J.; Scherman, O. A.; Abell, C. One-Step Fabrication of Supramolecular Microcapsules From Microfluidic Droplets. *Science* **2012**, *335*, 690−694.
(19) Pawar, A. B.; Caggioni, M.; Ergun, R.; Hartel, R. W.; Spicer, P. T. Arrested Coalescence in Pickering Emulsions. *Soft Matter* **2011**, *7*, 7710−7716.
(20) He, J.; Zhang, Q.; Gupta, S.; Emrick, T.; Russell, T. P.; Thiyagarajan, P. Drying Droplets: a Window Into the Behavior of Nanorods at Interfaces. *Small* **2007**, *3*, 1214−1217.
(21) He, J.; Kanjanaboos, P.; Frazer, N. L.; Weis, A.; Lin, X.-M.; Jaeger, H. M. Fabrication and Mechanical Properties of Large-Scale Freestanding Nanoparticle Membranes. *Small* **2010**, *6*, 1449−1456.
(22) Costa, L.; Li-Destri, G.; Thomson, N. H.; Konovalov, O.; Pontoni, D. Real Space Imaging of Nanoparticle Assembly at Liquid−Liquid Interfaces with Nanoscale Resolution. *Nano Lett.* **2016**, *16*, 5463−5468.
(23) Bera, M. K.; Chan, H.; Moyano, D. F.; Yu, H.; Tatur, S.; Amoanu, D.; Bu, W.; Rotello, V. M.; Meron, M.; Král, P.; Lin, B.; Schlossman, M. L. Interfacial Localization and Voltage-Tunable Arrays of Charged Nanoparticles. *Nano Lett.* **2014**, *14*, 6816−6822.
(24) Pickering, S. U. CXCVI.—Emulsions. *J. Chem. Soc., Trans.* **1907**, *91*, 2001−2021.
(25) Pieranski, P.; Srezelecki, L.; Pansu, B. Thin Colloidal Crystals. *Phys. Rev. Lett.* **1983**, *50*, 900−903.
(26) Pieranski, P. Two-Dimensional Interfacial Colloidal Crystals. *Phys. Rev. Lett.* **1980**, *45*, 569−572.
(27) Binks, B. P.; Lumsdon, S. O. Influence of Particle Wettability on the Type and Stability of Surfactant-Free Emulsions †. *Langmuir* **2000**, *16*, 8622−8631.
(28) Dinsmore, A. D.; Hsu, M. F.; Nikolaides, M. G.; Marquez, M.; Bausch, A. R.; Weitz, D. A. Colloidosomes: Selectively Permeable Capsules Composed of Colloidal Particles. *Science* **2002**, *298*, 1006−1009.
(29) Binks, B. P. Particles as Surfactants—Similarities and Differences. *Curr. Opin. Colloid Interface Sci.* **2002**, *7*, 21−41.
(30) Niu, Z.; He, J.; Russell, T. P.; Wang, Q. Synthesis of Nano/Microstructures at Fluid Interfaces. *Angew. Chem., Int. Ed.* **2010**, *49*, 10052−10066.
(31) Garbin, V.; Crocker, J. C.; Stebe, K. J. Forced Desorption of Nanoparticles From an Oil−Water Interface. *Langmuir* **2012**, *28*, 1663−1667.
(32) Lohmeijer, B. G. G.; Dubois, G.; Leibfarth, F.; Pratt, R. C.; Nederberg, F.; Nelson, A.; Waymouth, R. M.; Wade, C.; Hedrick, J. L. Organocatalytic Living Ring-Opening Polymerization of Cyclic Carbosiloxanes. *Org. Lett.* **2006**, *8*, 4683−4686.
(33) Bae, J.; Russell, T. P.; Hayward, R. C. Osmotically Driven Formation of Double Emulsions Stabilized by Amphiphilic Block Copolymers. *Angew. Chem., Int. Ed.* **2014**, *53*, 8240−8245.
(34) Erni, P. Deformation Modes of Complex Fluid Interfaces. *Soft Matter* **2011**, *7*, 7586−7600.
(35) Ravera, F.; Ferrari, M.; Liggieri, L.; Loglio, G.; Santini, E.; Zanobini, A. Liquid−Liquid Interfacial Properties of Mixed Nanoparticle−Surfactant Systems. *Colloids Surf., A* **2008**, *323*, 99−108.
(36) Ravera, F.; Loglio, G.; Kovalchuk, V. I. Interfacial Dilational Rheology by Oscillating Bubble/Drop Methods. *Curr. Opin. Colloid Interface Sci.* **2010**, *15*, 217−228.
(37) Alvarez, N. J.; Anna, S. L.; Saigal, T.; Tilton, R. D.; Walker, L. M. Interfacial Dynamics and Rheology of Polymer-Grafted Nanoparticles at Air−Water and Xylene−Water Interfaces. *Langmuir* **2012**, *28*, 8052−8063.
(38) Reichert, M. D.; Alvarez, N. J.; Brooks, C. F.; Grillet, A. M.; Mondy, L. A.; Anna, S. L.; Walker, L. M. Colloids and Surfaces a: Physicochemical and Engineering Aspects. *Colloids Surf., A* **2015**, *467*, 135−142.
(39) Feng, T.; Hoagland, D. A.; Russell, T. P. Interfacial Rheology of Polymer/Carbon Nanotube Films Co-Assembled at the Oil/Water Interface. *Soft Matter* **2016**, *12*, 1−9.
(40) Lohmeijer, B. G. G.; Dubois, G.; Leibfarth, F.; Pratt, R. C.; Nederberg, F.; Nelson, A.; Waymouth, R. M.; Wade, C.; Hedrick, J. L. Organocatalytic Living Ring-Opening Polymerization of Cyclic Carbosiloxanes. *Org. Lett.* **2006**, *8*, 4683−4686.
(41) Voet, V. S. D.; Pick, T. E.; Park, S.-M.; Moritz, M.; Hammack, A. T.; Urban, J. J.; Ogletree, D. F.; Olynick, D. L.; Helms, B. A. Interface Segregating Fluoralkyl-Modified Polymers for High-Fidelity Block Copolymer Nanoimprint Lithography. *J. Am. Chem. Soc.* **2011**, *133*, 2812−2815.

DOI: 10.1021/acs.langmuir.7b01685
Langmuir 2017, 33, 7994−8001